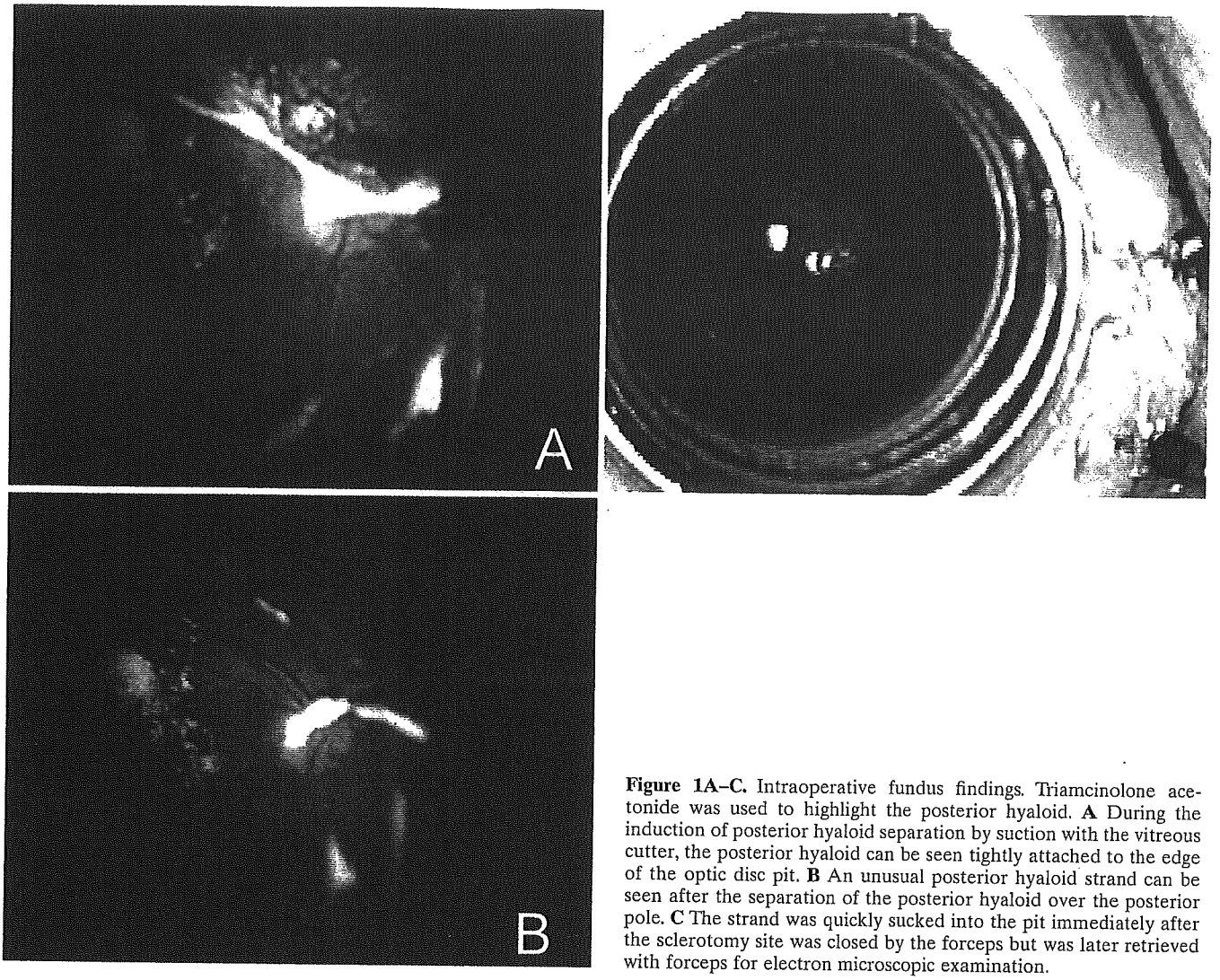

Figure 1A–C. Intraoperative fundus findings. Triamcinolone acetonide was used to highlight the posterior hyaloid. **A** During the induction of posterior hyaloid separation by suction with the vitreous cutter, the posterior hyaloid can be seen tightly attached to the edge of the optic disc pit. **B** An unusual posterior hyaloid strand can be seen after the separation of the posterior hyaloid over the posterior pole. **C** The strand was quickly sucked into the pit immediately after the sclerotomy site was closed by the forceps but was later retrieved with forceps for electron microscopic examination.

corrected visual acuity (VA) in the left eye was 0.08. An optic disc pit was detected on the temporal side of the optic disc, associated with an oval-shaped, shallow macular detachment covering the area between the superior and inferior vessel arcade. The macular detachment appeared to communicate with the pit. A round, two-disc diameter, serous retinal detachment was observed in the center of the macula, with cystic changes. OCT (Zeiss-Humphrey, San Leandro, CA, USA) revealed a separation of the inner retinal layers that appeared to connect with the optic disc, as well as a defect in the outer layer at the macula and a detachment surrounding the hole.

Because of the progression of the macular detachment and the enlargement of the outer macular hole over the next 4 months, we decided to perform vitrectomy. Informed consent was obtained from the parents after an explanation of the procedures and prognosis. The use of TA intraoperatively enabled us to clearly visualize the posterior hyaloid membrane. During the induction of the posterior vitreous detachment (PVD), a hyaloid strand was detected tightly adhering to the margin of the disc pit (Fig. 1A). Part of the strand was left attached to the edge of the pit after the removal of the posterior hyaloid membrane over the posterior pole with a vitreous cutter (Fig. 1B). As the vitreous forceps was inserted through the sclerotomy site to grasp the strand at the pit, the strand was quickly sucked into the pit and almost disappeared (Fig. 1C). The strand was pulled out of the pit with the vitreous forceps and removed. Fluid–air exchange was performed followed by gas tamponade with 20% SF_6.

The patient's VA began to improve 1 month postoperatively, corresponding to the improvement in the retinoschisis and macular serous detachment. At 6 months postoperatively, the VA was 0.8. OCT performed at 9 months postoperatively showed resolution of the retinoschisis, but the serous detachment was still present. By 12 months, the VA was 1.2, and funduscopy and OCT showed a complete reattachment of the retina.

Electron microscopic examination of the excised specimen revealed abundant clusters of collagen fibers with a frame of fine fibrils (Fig. 2A). Most of the collagen fibrils, which appeared to be type I collagen, were 15 to 25 nm in

Jpn J Ophthalmol
Vol 49: 264–266, 2005

Figure 2A,B. Electron photomicrographs of the excised specimen. **A** Electron microscopic examination shows clusters of collagen fibers with a frame of fine fibrils. Very few cells are present. Bar = 1.0 μm. **B** Under higher magnification, most of the collagen fibrils, which appear to be type I collagen, were 15 to 25 nm in diameter with a regular periodicity of 45–55 nm. Bar = 0.1 μm.

diameter with a regular periodicity of 45–55 nm (Fig. 2B). Very few cells were present in the specimen.

Discussion

Recent OCT findings have revealed that the macular detachment associated with an optic disc pit consists of a bilaminar structure. However, the mechanism responsible for the macular serous detachment remains unclear. Bonnet[5] reported that none of 25 eyes with macular serous detachment associated with an optic disc pit initially had a PVD, and two of the eyes had a spontaneous reattachment of the macula following the development of a PVD. Several investigators have discussed the efficacy of vitrectomy and gas tamponade to treat optic disc pit maculopathy.[3–5] In our studies, vitrectomy using modern surgical techniques to create a PVD in young patients and gas tamponade without laser photocoagulation were successful in reattachment of the macula with an improvement in central vision in 10 out of 11 eyes with optic disc pit maculopathy. However, most of the eyes required almost 1 year of recovery to attain this state (submitted for publication). These observations support the concept that vitreous traction may have an important role in the development of macular detachment associated with optic disc pits.

Akiba and coauthors[2] reported that 11 out of 15 eyes with optic pit maculopathy without a PVD had an anomalous Cloquet's canal that was markedly condensed and terminated at the margin of the pit. During ocular movements, they observed a back-and-forth movement of the anomalous Cloquet's canal and a pulsating translucent membrane that covered the pit. Several case reports have described similar abnormal structures anterior to the pit, based on scanning laser ophthalmoscopic observations or intraoperative findings.[3,4]

The intraoperative use of TA to observe the posterior hyaloid appears to be a useful technique to detect abnormal adhesions of the vitreous to the margin of the disc pit, as in our case. The peculiar sucking of the strand into the pit during the insertion of the vitreous forceps into the eye suggests that the optic disc pit may connect to the subarachnoid space, resulting in suction from the subarachnoid space produced by an imbalance between the intraocular and the subarachnoid pressures.

Histological examination of the posterior hyaloid strand that was connected to the pit showed abundant clusters of thick collagen fibers with a frame of fine fibrils and very few cells. This feature of collagen is different from that found in the native vitreous collagen, and is consistent with the observations of previous reports[2–4] describing the presence of condensed membranes in anomalous Cloquet's canals attached to optic disc pits. However, we did not observe similar vitreous strands in most of the eyes with optic disc pit maculopathy in our clinical series.

Patient age at the onset of the retinal detachment associated with optic disc pits is variable, with a mean age of 30 years. Our present patient was exceptionally young, suggesting that unusual posterior vitreous strands connected to the optic disc pit might contribute to the pathogenesis of maculopathy in some patients with optic disk pit.

References

1. Rutledge BK, Puliafito CA, Duker JS, Hee MR, Cox MS. Optical coherence tomography of macular lesions associated with optic nerve head pits. Ophthalmology 1996;103:1047–1053.
2. Akiba J, Kakehashi A, Hikichi T, Trempe CL. Vitreous findings in cases of optic nerve pits and serous macular detachment. Am J Ophthalmol 1993;116:38–41.
3. Hasegawa T, Akiba J, Ishiko S, et al. Abnormal vitreous structure in optic nerve pit. Jpn J Ophthalmol 1997;41:324–327.
4. Seki K, Takahashi H, Sato Y. A case of pit-macular syndrome with a plicated membrane identified during vitrectomy. Ganka (Ophthalmology) 2001;43:793–798.
5. Bonnet M. Serous macular detachment associated with optic nerve pits. Graefes Arch Clin Exp Ophthalmol 1991;229:526–532.

Jpn J Ophthalmol 2006;50:53–61

DOI 10.1007/s10384-005-0270-4

CLINICAL INVESTIGATION

Vitrectomy for Myopic Posterior Retinoschisis or Foveal Detachment

Akito Hirakata and Tetsuo Hida

Kyorin Eye Center, Kyorin University School of Medicine, Mitaka, Tokyo, Japan

Abstract

Purpose: To evaluate the efficacy of vitrectomy for posterior retinoschisis (RS) or foveal detachment (FD) associated with posterior staphyloma in myopic eyes.

Methods: We reviewed the records of 14 consecutive patients (53–77 years of age; 16 eyes) with progressive visual impairment as a result of myopic RS or FD. Optical coherence tomography demonstrated the presence of a variety of RS and FD characteristics. Five eyes had RS alone, and 11 eyes had RS and FD. Two eyes with RS and severe FD developed retinal detachment in conjunction with a tiny macular hole. Vitrectomy, including posterior vitreous separation in all eyes and internal limiting membrane (ILM) peeling in six eyes, had been performed. The patients were followed postoperatively for 6 to 66 months (mean, 24 months). The anatomical outcome and visual acuity were retrospectively analyzed in this study.

Results: Although the two eyes with RS and severe FD developed retinal detachment with a macular hole after an initial vitrectomy, final retinal reattachment was achieved in all 16 eyes. Visual acuity improved in nine eyes and remained unchanged in seven eyes.

Conclusions: Vitrectomy with posterior vitreous separation is effective for reattaching the macula and preventing a deterioration of vision, although eyes with RS and severe FD may be at risk for the development of a macular hole after the initial vitrectomy. **Jpn J Ophthalmol** 2006;50:53–61 © Japanese Ophthalmological Society 2006

Key Words: high myopia, macular detachment, optical coherence tomography, retinoschisis, vitrectomy

Introduction

Posterior retinal detachment associated with a macular hole is a well-known complication in highly myopic eyes with posterior staphyloma. However, localized shallow posterior retinal detachment inside posterior staphyloma can also exist in the absence of a macular hole. In 1958, Phillips noted that localized posterior retinal detachment over posterior staphyloma might occur in the absence of a retinal hole.[1] Using optical coherence tomography (OCT), Takano and Kishi[2] reported that foveal retinoschisis or foveal retinal detachment occurs frequently in severely myopic eyes with posterior staphyloma, even in the absence of a macular hole. They suggested that retinal detachment may precede the formation of a macular hole in highly myopic eyes. However, the pathological mechanism responsible for posterior retinoschisis and the process of macular hole development are not well understood.

Recently, several authors have reported that vitrectomy, internal limiting membrane (ILM) peeling, and gas tamponade are useful for the treatment of foveal retinoschisis in highly myopic eyes.[3–7] Kobayashi and Kishi[4] also suggested that vitreous surgery might be indicated as a prophylactic treatment in highly myopic eyes at high risk for macular hole development. However, myopic foveal retinoschisis exhibits a variety of profiles,[8,9] and the accumulated data on surgical cases remain insufficient to prove

Received: October 12, 2004 / Accepted: May 2, 2005
Correspondence and reprint requests to: Akito Hirakata, Department of Ophthalmology, Kyorin University School of Medicine, 6-20-2 Shinkawa, Mitaka, Tokyo 181-8611, Japan
e-mail: hirakata@eye-center.org

Jpn J Ophthalmol
Vol 50: 53–61, 2006

whether vitrectomy is effective for the alleviation of this condition.

The purpose of the present study was to examine the clinical outcomes of vitrectomies performed in the Kyorin University Hospital between September 1998 and February 2004 in 14 consecutive patients (16 eyes) with localized shallow posterior retinal detachment inside a posterior staphyloma who exhibited signs of progressive visual impairment. Different clinical terms have been used to describe this pathological condition in previous reports, including foveal retinoschisis,[2] foveal detachment and retinoschisis,[2,4] macular retinoschisis,[5,9] shallow detachment of the macula,[1] and foveal retinal detachment without a macular hole.[8] In this paper, we use the terms posterior retinoschisis (RS) and foveal detachment (FD) to describe this pathological condition.

Patients and Methods

Fourteen consecutive patients (16 eyes) with myopia and posterior staphyloma who exhibited progressive visual impairment as a result of RS or FD were included in this study. Their records were retrospectively reviewed. Informed consent had been obtained from all study patients. The fundus of each patient had been pre- and postoperatively examined by indirect ophthalmoscopy and slit-lamp biomicroscopy using a Goldmann contact lens and a 90-diopter noncontact fundus examination lens (SuperField Lens). The best-corrected visual acuity (BCVA) was recorded. An OCT system (Zeiss-Humphrey, San Leandro, CA, USA) had been used to observe the posterior retinal changes. In this study the anatomical outcome and BCVA were retrospectively analyzed for all eyes.

Surgery had been initiated once the patient's vision had begun to deteriorate and the macular detachment had persisted or progressed for 3 months or longer. Two eyes (cases 13, 14) with RS and severe FD developed retinal detachment with a tiny macular hole before the vitrectomy. All the operations were performed by the same surgeon (AH) between September 1998 and February 2004. Vitrectomy, including posterior vitreous cortex removal from the retinal surface, was performed in all eyes, and ILM peeling was performed in six eyes. After core vitrectomy, complete removal of the posterior vitreous cortex (typically appearing as a thin membrane) from the posterior retinal surface was initiated by cutting with a microvitreoretinal knife (20-gauge) or a diamond-dusted membrane scraper.[10] A viscodissection technique[11] was used to advance the posterior hyaloid separation gently over the areas of retinoschisis in the posterior staphyloma. Triamcinolone acetonide (TA) was used intraoperatively in five cases to highlight the posterior hyaloid membrane.[12] ILM peeling over the posterior pole was regarded as indicated in eyes in which the presence of posterior hyaloid separation or induction over the macula was uncertain during the vitreous surgery, and was performed after indocyanine green (ICG) staining (5 mg/ml) in six eyes. In 12 eyes, fluid–air exchange was carried out without drainage of the subretinal fluid, followed by gas tamponade with either 20% sulfur hexafluoride (SF_6) or 14% perfluoropropane (C_3F_8). The patients were placed in a facedown position postoperatively. In two eyes [patients 5 (right eye, R) and 10], silicone oil tamponade was used because of poor vision in the opposite eye.

Twelve eyes were phakic before surgery, and four eyes had received phacoemulsification with intraocular lens implantation for the treatment of senile cataracts. Among the 12 phakic eyes, phacoemulsification with intraocular lens implantation was performed simultaneously with the vitrectomy in two eyes, and after the vitrectomy in six eyes.

The patients were followed for 6 to 66 months (mean, 24 months) after surgery.

Results

Case Reports

Patient 1

A 59-year-old man presented with a history of several months of metamorphopsia in his right eye. He also had a

Figure 1A–C. Fundus photograph and optical coherence tomography (OCT) images of the right eye of patient 1. **A** A photograph taken at presentation in an eye with a best-corrected visual acuity (BCVA) of 0.5 and metamorphopsia shows a shallow macular detachment over the posterior staphyloma. **B** An OCT examination confirmed the foveal detachment and posterior retinoschisis (scan length, 5.0 mm). **C** About 4 years after the operation, the BCVA had improved to 0.7. An OCT image shows complete reattachment (scan length, 5.0 mm).

Figure 2A–D. Fundus photograph and OCT images of the right eye of patient 2. **A** During a routine follow-up for macular hole retinal detachment in the left eye, the BCVA of the right eye was found to have decreased from 0.8 to 0.5. The fundus photograph shows a shallow macular detachment. **B** A preoperative OCT image shows a shallow elevation of the macula without splitting of the fovea, creating the appearance of a lamellar hole (scan length, 5.0 mm). **C** Two months after the vitrectomy, an OCT image shows a marked resolution of the retinoschisis (scan length, 3.5 mm). **D** At 4 years postoperatively, the retina had completely reattached (scan length, 10.0 mm).

Figure 3A–C. Fundus photograph and OCT images of the right eye of patient 11. **A** A preoperative fundus photograph shows a shallow retinal elevation over a posterior staphyloma in an eye with a BCVA of 0.4. **B** A preoperative OCT image shows an inner layer separation that appears to be connected to the conus of the optic disc (1), as well as to a large outer layer detachment at the macula (2). A partial posterior hyaloid separation surrounding the posterior retinoschisis is visible (scan length, 10.0 mm). **C** At 6 months after the vitrectomy, an OCT image shows a marked improvement of the retinal detachment (scan length, 10.0 mm).

Figure 4A–C. Fundus photograph and OCT images of the left eye of patient 5. **A** A preoperative fundus photograph shows a shallow retinal elevation over a posterior staphyloma. The BCVA of the eye was 0.06. **B** An OCT image shows a posterior retinoschisis over the posterior staphyloma, with a partial separation of the posterior hyaloid. Outer layer detachment is not visible (scan length, 10.0 mm). **C** Two weeks after the vitrectomy, the retina had completely reattached (scan length, 10.0 mm).

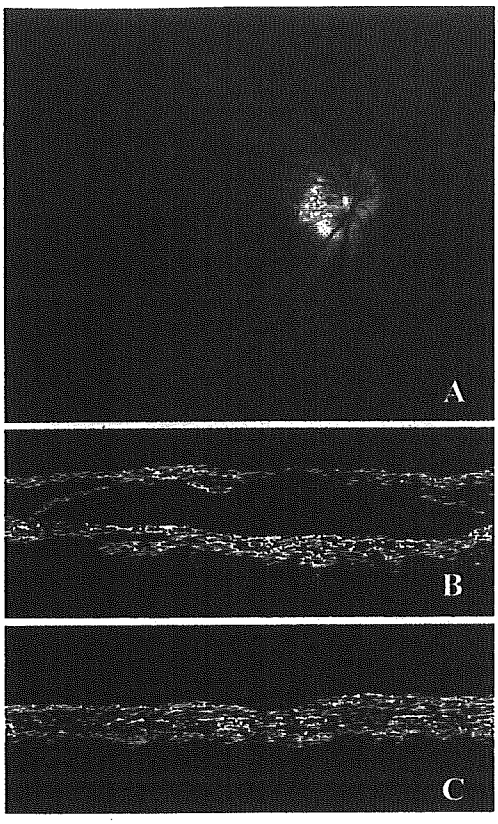

Figure 1

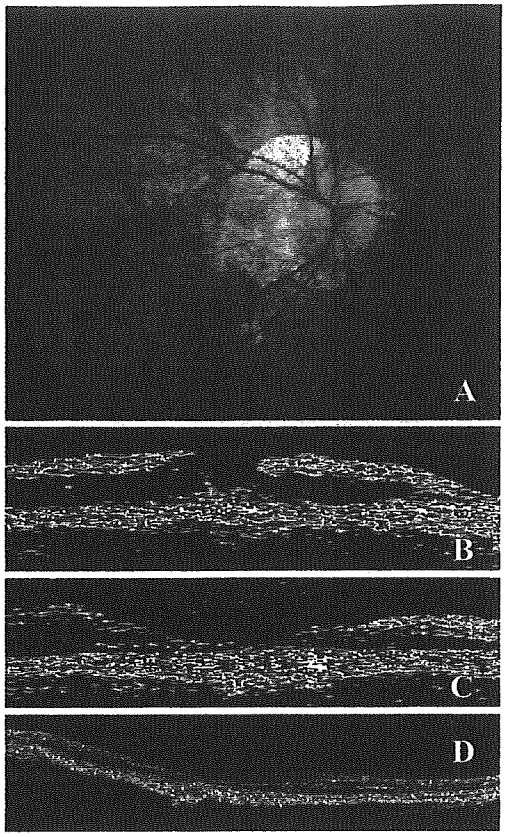

Figure 2

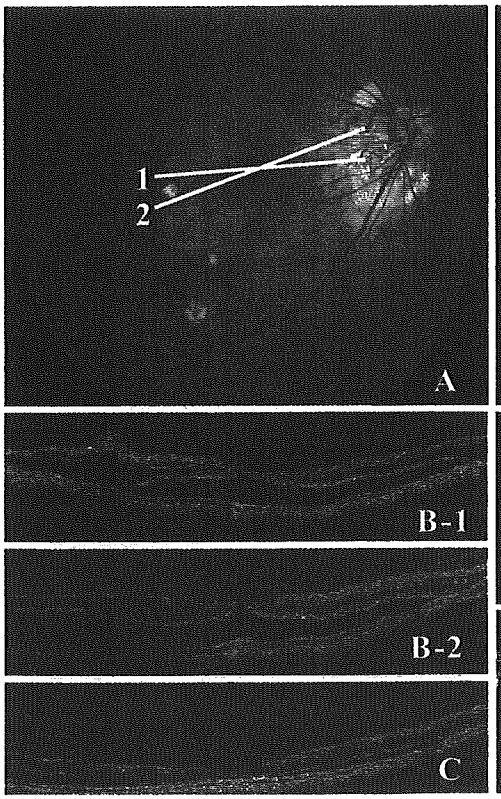

Figure 3

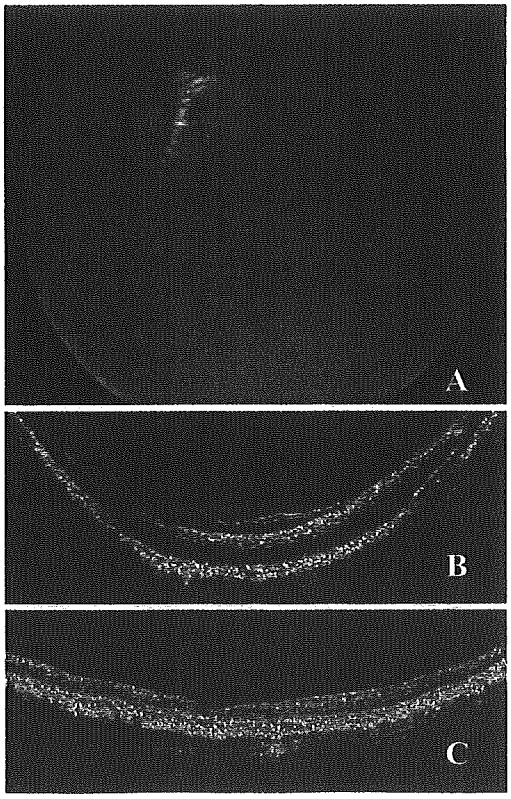

Figure 4

history of von Recklinghausen disease and refractive amblyopia. Examination of the right eye revealed a BCVA of 0.5 and a shallow serous macular detachment over the posterior staphyloma (Fig. 1A). OCT confirmed the presence of FD and RS (Fig. 1B).

After the patient had been observed for 3 months, he complained of increasing metamorphopsia, although an examination of his vision revealed no change. Vitrectomy was performed, with removal of the posterior hyaloid membrane and ILM peeling by viscodissection, followed by air–fluid exchange and 14% C_3F_8 gas tamponade.

Two months postoperatively, the BCVA was 0.6, and an OCT examination showed a marked resolution of the retinal detachment. The patient reported an improvement in the metamorphopsia. Six months postoperatively, the patient developed nuclear sclerosis of the lens, so phacoemulsification with intraocular lens implantation was performed. Consequently, the patient's BCVA further improved to 0.7. The posterior retina was found to be completely reattached, with no further changes during a 54-month follow-up examination. An OCT examination about 4 years later revealed a nearly normal configuration of the fovea (Fig. 1C).

Patient 2

A 53-year-old woman with a history of vitrectomy for a macular hole retinal detachment in her left eye 3 years earlier was noted to have a shallow elevation of the macula in her asymptomatic right eye during a routine follow-up examination. OCT revealed RS in the right eye.

One year later, she complained of a slight decrease in central vision and metamorphopsia in her right eye. Although her visual acuity had decreased from 0.8 to 0.4, a fundus examination showed no obvious changes in the severity of the RS (Figs. 2A, B). Vitrectomy and phacoemulsification with intraocular lens implantation were performed. Intraoperatively, marked syneresis of the vitreous was observed. Following core vitrectomy, we were able to easily induce posterior vitreous detachment (PVD) by suctioning with the vitreous cutter everywhere except over the posterior pole; ILM peeling was necessary to ensure the complete removal of the posterior hyaloid inside the staphyloma. Fluid–air exchange without subretinal drainage was performed, followed by gas tamponade with 14% C_3F_8. Two months after surgery, the patient reported that her metamorphopsia had diminished. An OCT examination showed a marked resolution of the RS (Fig. 2C). Six months after surgery, although the BCVA remained unchanged at 0.5, the patient reported an improvement in the metamorphopsia. Four years after the operation, an OCT examination confirmed the complete reattachment of the retina (Fig. 2D), and the patient's BCVA had been restored to 0.8.

Patient 11

A 70-year-old woman with a history of phacoemulsification with intraocular lens implantation complained of a 4-month history of metamorphopsia in her right eye. The patient's BCVA was 0.4, and a shallow retinal elevation was noted extending from the superotemporal to the inferotemporal arcades over posterior staphyloma (Fig. 3A). No retinal breaks were detected. OCT revealed an RS that appeared to be connected to the conus of the optic disc, as well as a large outer layer detachment at the macula and a partial posterior hyaloid separation surrounding the RS (Fig. 3B).

Vitrectomy and 20% SF_6 gas tamponade was performed with the adjunctive use of TA intraoperatively. The use of TA to observe the posterior hyaloid intraoperatively appears to be a useful technique when attempting to completely separate tight adhesions to the retina. One month after the surgery, the patient reported that her metamorphopsia had diminished. The patient's BCVA was 0.5, and an OCT examination showed a marked improvement in the inner layer separation and outer layer detachment. At 6 months after the operation, an OCT examination showed complete retinal reattachment (Fig. 3C). One year after the operation, the BCVA had been restored to 0.7.

Preoperative Clinical Characteristics

The clinical characteristics of all 14 patients are shown in Table 1. Eleven patients were women and three were men, and they ranged in age from 53 to 77 years (mean ± SD, 64.8 ± 7.7 years). All the patients were healthy and of Japanese ancestry, and all had complained of metamorphopsia or reduced vision in the affected eye for several months. The refractive errors ranged from −6.0 to −19.25 diopters (mean ± SD, −13.2 ± 3.8 D) in 12 phakic eyes. The axial lengths ranged from 24.9 to 30.4 mm (mean ± SD, 27.6 ± 1.6 mm). The eye of patient 7 was not highly myopic, but posterior staphyloma and glaucomatous cupping of the optic disc were present. The posterior staphyloma extended over a wide area in all 16 eyes. The decimal preoperative visual acuity values ranged from 0.01 to 0.5 (mean, 0.14).

OCT examinations disclosed various profiles of macular change. The presence of RS or FD was confirmed preoperatively in all eyes. Five eyes had RS alone. In four of these eyes, an extensive hyporefractive space had split the retina into a thick inner layer and a thin outer layer lying on the retinal pigment epithelium (RPE) [patients 1 (left eye, L), 3, 5 (R), and 6] (Fig. 4A, B). One eye (patient 2) had a similar appearance, but the fovea was not split and did not show a defect in the roof of the central cyst, giving the appearance of a lamellar hole (Fig. 2B). The BCVA in four of the five eyes with RS without FD was better than 0.2.

Eleven eyes had RS associated with FD (Figs. 1B, 3B, 5B). The BCVA of these eyes seemed to be worse than that

Table 1. Clinical characteristics

Patient	Age (years)	Sex	Eye	Ref (D)	Axial length (mm)	Symptom	Preoperative BCVA	OCT finding		Intraoperative finding			Final attachment	Final BCVA	Complications	Follow-up (months)	Fellow eye
								RS/FD	PVD	PVD Ind.	ILM peel	Tamp					
1	59	M	L	−8.75	26.7	Decreased VA	0.06	RS	—	+	−	C_3F_8	+	0.2	—	66	RS,FD
			R	−11.00	27.0	Decreased VA	0.5	RS,FD	—	+	+	C_3F_8	+	0.7	—	54	RS
2	53	F	R	−19.25	28.7	Metamorphopsia	0.4	RS	—	+	+	C_3F_8	+	0.8	—	52	MHRD
3	72	F	R	−9.75	27.9	Metamorphopsia	0.4	RS	—	+	+	—	+	0.8	—	45	—
4	75	F	R	IOL	26.2	VF defect	0.01	RS,FD	—	+	+	C_2F_8	+	0.07	MH	17	—
5	68	F	L	−15.00	27.5	Decreased VA	0.06	RS,FD	Part	+	−	SF_6	+	0.06	RRD	16	RS
			R	−17.75	30.0	Metamorphopsia	0.2	RS	Part	+	−	SO	+	0.6	Retinal break	10	RS,FD
6	63	F	L	−12.5	29.2	Metamorphopsia	0.4	RS	—	+	−	—	+	0.4	—	27	—
7	63	M	L	−6.0	24.9	Decreased VA	0.1	RS,FD	—	+	+	SF_6	+	0.5	—	27	Gla
8	54	F	R	−15.00	27.0	Metamorphopsia	0.01	RS,FD	Part	+	+	SF_6	+	0.1	MHRD	22	—
9	56	F	L	−14.00	29.2	Decreased VA	0.2	RS,FD	Part	+	−	SF_6	+	0.1	MHRD	17	RS,FD
10	77	F	L	IOL	27.4	Metamorphopsia	0.3	RS,FD	Part	+	−	SO	+	0.3	—	15	MHRD
11	70	F	R	IOL	30.2	Metamorphopsia	0.4	RS,FD	Part	+	−	SF_6	+	0.7	—	13	—
12	74	F	R	IOL	29.9	VF defect	0.06	RS,FD	Part	+	−	SF_6	+	0.2	—	6	RS
13	66	M	L	−15.00	29.6	Decreased VA	0.3→0.1	RS,FD→ MHRD	—	+	−	C_3F_8	+	0.2	MH	11	MHRD
14	59	F	R	−19.00	30.4	Decreased VA	0.2→0.06	RS,FD→ MHRD	—	+	−	C_3F_8	+	0.4	MH	12	—

BCVA, best-corrected visual acuity; C_3F_8, perfluoropropane; D, diopter; F, female; FD, foveal detachment; Gla, glaucoma; ILM, internal limiting membrane; Ind, induction; IOL, intraocular lens; L, left; M, male; MH, macular hole; MHRD, macular hole retinal detachment; OCT, optical computed tomography; Part, partial detachment; PVD, posterior vitreous detachment; R, right; Ref, refractive error; RRD, rhegmatogenous retinal detachment; RS, retinoschisis; SO, silicone oil; SF_6, sulfur hexafluoride; Tamp, tamponade; VA, visual acuity; VF, visual field.

of the eyes without FD, but 6 of the 11 eyes with FD had a BCVA that was better than 0.2. Two eyes developed macular hole retinal detachment during the routine follow-up period, and the BCVA decreased from 0.3 to 0.1 in patient 13 and from 0.2 to 0.06 in patient 14. Figures 6 and 7 show the changes in the macular configurations associated with the reduction in BCVA during the follow-up period in patients 13 and 14.

The presence of a partially detached posterior hyaloid was disclosed in seven eyes (Figs. 3, 4, 5). The separation of the posterior hyaloid beside the conus of the optic disc was observed in all of these seven eyes. Advanced vitreous syneresis was observed in all of these eyes, but PVD was not observed in the other nine eyes preoperatively.

Regarding the fellow eyes of the patients, three patients had a medical history of macular hole detachment, five patients had a history of RS and/or FD, one patient had a history of myopic posterior chorioretinal atrophy, and one patient had a history of primary open-angle glaucoma.

Anatomical Results

In all five eyes that had RS without FD, the retina reattached after the initial vitrectomy. Retinal reattachment was achieved in 8 out of 11 eyes with both RS and FD, including two cases that had progressed to macular hole retinal detachment (patients 13 and 14) before the initial vitrectomy. We removed the silicone oil about 5 and 2 months after the vitrectomies in patients 5 (R) and 10, respectively. The retina remained reattached after the removal.

Three eyes required reoperation because of recurrent retinal detachment. In two of these three eyes, a full-thickness macular hole associated with posterior retinal detachment occurred 1 month after vitrectomy with (patient 8) and without ILM peeling (patient 9; Fig. 8). We performed a second operation, consisting of extensive ILM peeling and silicone oil tamponade. At 5 months (patient 8) and 3 months (patient 9) after the second surgery, we removed the silicone oil, and retinal reattachment was confirmed by OCT in both eyes. One eye (patient 5, L) developed retinal detachment caused by a peripheral retinal break immediately after the initial vitrectomy. A second vitrectomy was thus performed to repair the retinal detachment.

Final retinal reattachment was achieved in all 16 eyes. No recurrences were observed during follow-up.

Visual Acuity Results

An improvement in the BCVA of 0.2 logMAR or greater was documented in 9 of the 16 eyes. The BCVA of seven eyes remained unchanged. The BCVA of the left eye of patient 5 improved from 0.06 to 0.1 at 12 months after the vitrectomy, but decreased again to 0.06 at 16 months, with no remarkable changes in the retinal findings. During this follow-up period, we performed a vitrectomy for the treat-

Jpn J Ophthalmol
Vol 50: 53–61, 2006

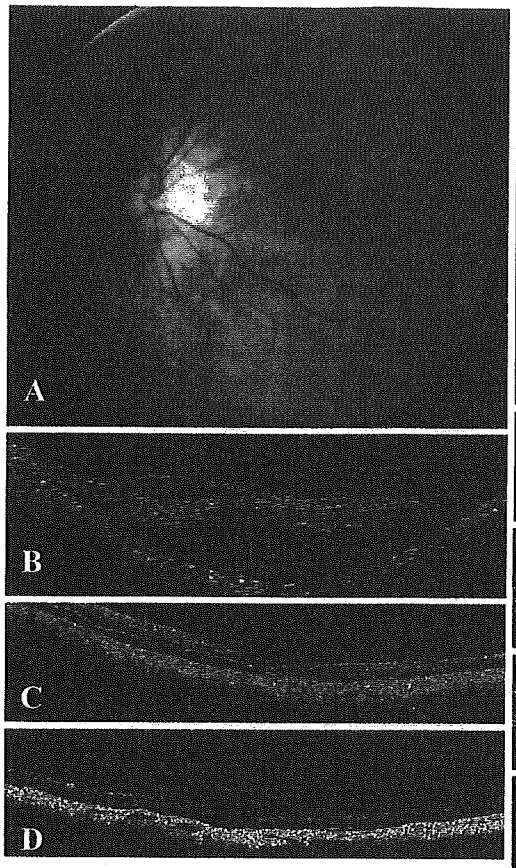

Figure 5

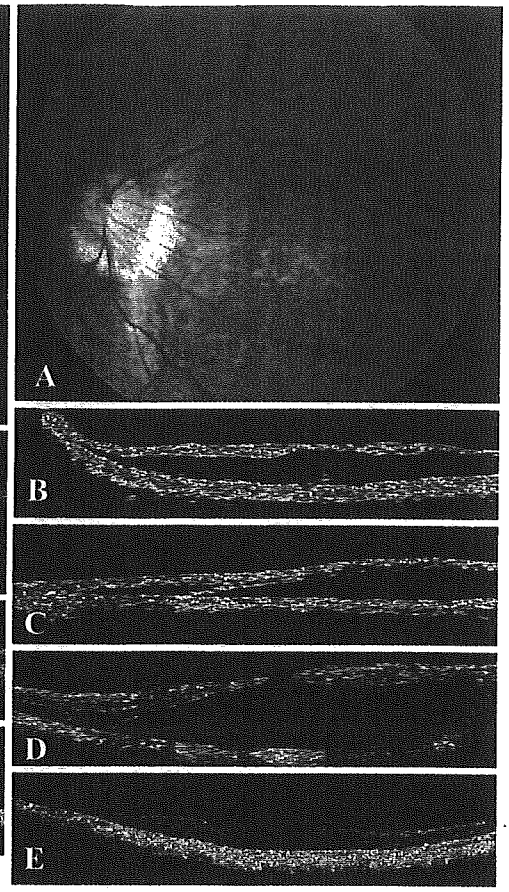

Figure 6

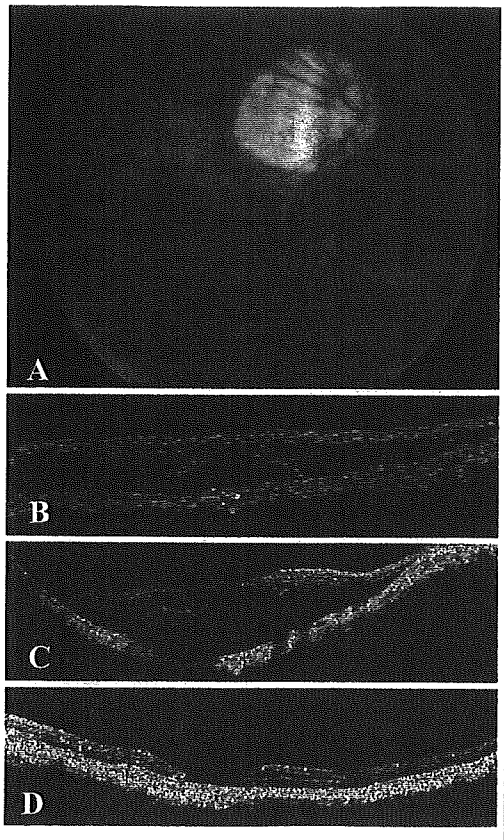

Figure 7

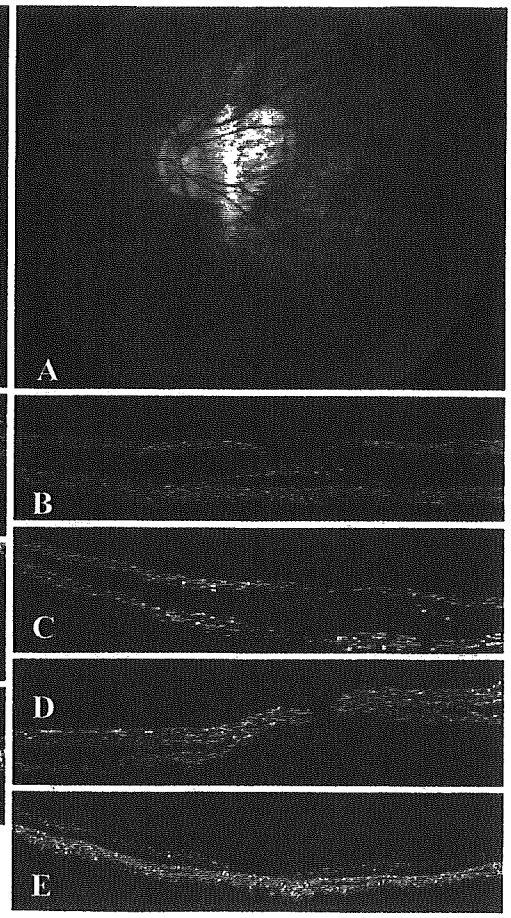

Figure 8

ment of RS in the right eye, which resulted in an improvement of VA from 0.2 to 0.6.

Fourteen of the 16 eyes had a final VA of 0.1 or better, and six eyes had a BCVA of better than 0.5.

Complications

Intraoperative or postoperative complications were observed in seven eyes. The retina redetached in three eyes [patients 5 (L), 8, and 9], as described above.

A full-thickness macular hole was observed after the initial vitrectomy in 5 of the 16 eyes. In four of these five eyes, the full-thickness macular hole associated with the retinal detachment appeared before (patients 13 and 14) or after the vitrectomy (patients 8 and 9), as described above. In the fifth eye (patient 4), a macular hole was found in the reattached retina after vitrectomy with ILM peeling and C_3F_8 gas tamponade. All five of these eyes had severe preoperative FD associated with RS and a poor VA.

Patient 5 developed a peripheral retinal break in the right eye intraoperatively during PVD induction that was treated successfully with laser photocoagulation.

Figure 5A–D. Fundus photograph and OCT images of the left eye of patient 10. **A** A preoperative fundus photograph shows a shallow macular detachment in an eye with a BCVA of 0.3. **B** A preoperative OCT image shows a marked elevation of the posterior retina. A posterior retinoschisis is visible from the edge of the conus of the optic disc to the edge of the posterior staphyloma. The outer layer detachment is remarkable. A partial separation of the posterior hyaloid is visible between the fovea and the conus of the optic disc (scan length, 9.0mm). **C** Two months after the vitrectomy, the posterior retina elevation was remarkably reduced (scan length, 10.0mm). **D** Fifteen months postoperatively, the retina had completely reattached (scan length, 10.0mm).

Figure 6A–E. Fundus photograph and OCT images of the left eye of patient 13. **A, B** A 66-year-old man with a history of macular hole retinal detachment surgery in the right eye was noted to have posterior retinoschisis of the asymptomatic left eye during a routine follow-up examination. The BCVA of the left eye was 0.5 (scan length, 9.0mm). **C** After observation for 20 months, an OCT examination revealed the development of a foveal detachment associated with the posterior retinoschisis. The BCVA had decreased to 0.3, but the patient had not noticed the development of any visual disturbance (scan length, 9.0mm). **D** After observation for 30 months, he complained of reduced vision and scored a BCVA of 0.1. An OCT examination revealed a posterior retinal detachment associated with a macular hole, and vitrectomy was performed (scan length, 10.0mm). **E** Ten months postoperatively, the retina had completely reattached, but the macular hole persisted (scan length, 5.0mm).

Figure 7A–D. Fundus photograph and OCT images of the right eye of patient 14. **A** A fundus photograph taken at presentation shows a shallow posterior detachment over a posterior staphyloma in an eye with a BCVA of 0.5. **B** An OCT image taken at presentation shows a foveal detachment with posterior retinoschisis (scan length, 9.0mm). **C** Three months after presentation, the BCVA had decreased to 0.06; an OCT image shows macular hole retinal detachment. A vitrectomy was performed (scan length, 10.0mm). **D** Three months after the operation, an OCT image shows complete retinal reattachment, but the macular hole remains visible (scan length, 5.0mm).

Figure 8A–E. Fundus photograph and OCT images of the left eye of patient 9. **A** A preoperative fundus photograph shows a shallow posterior detachment over a posterior staphyloma in an eye with a BCVA of 0.2. **B** A preoperative OCT image shows posterior retinoschisis and foveal detachment (scan length, 2.8mm). **C** Two weeks after the vitrectomy, the posterior retinoschisis elevation has decreased, but foveal detachment has increased (scan length, 5.0mm). **D** One month after the vitrectomy, the patient noticed a reduced BCVA. An OCT image shows the development of macular hole retinal detachment (scan length, 5.0mm). **E** About 1.5 years postoperatively, the retina had completely reattached, but the macular hole remained visible (scan length, 5.0mm).

Discussion

We confirmed that OCT is a very important tool for observing the pathological appearance of highly myopic eyes, as concluded in previous reports.[2–9] These previous reports also noted that RS and FD were not uncommon. Baba and associates[8] reported that none of seven patients with foveal retinal detachment complained of recent, progressive visual impairment. In addition, one case report described the spontaneous resolution of a myopic foveal retinoschisis.[13] Benhamou and associates[9] reported that this condition is fairly stable, in terms of visual acuity and retinal thickness, and changes slowly over time. In the present study, we studied eyes with RS and/or FD and progressive visual impairment. Fourteen of the 16 eyes exhibited a symptomatic visual impairment at the time of the initial patient visit, and the other two eyes were noted to have asymptomatic RS during routine follow-ups for the other eye, with subsequent visual impairment in the following few years. Two of the 11 eyes associated with FD developed macular hole retinal detachment during the preoperative follow-up period. The patients noticed an acute decrease in BCVA after the development of macular hole retinal detachment. In one eye, OCT revealed changes in the macular appearance during a follow-up examination, with no accompanying visual disturbance. This change detected by OCT and the symptomatic visual impairment associated with RS or FD may reflect the high risk of developing a macular hole.

A high incidence of macular hole retinal detachment in the opposite eye (in 3 out of 14 patients) and the preoperative progression leading to the development of macular hole retinal detachment in 2 out of the 16 eyes support the hypothesis of Takano et al.,[2] who suggested that RS and FD in highly myopic eyes may precede macular hole retinal detachment.

In this study, OCT examination revealed various macular profiles of myopic RS and FD, similar to the description by Benhamou et al.[9] RS involving the entire posterior pole connected to the conus of the optic disc was observed in all 16 cases; thus, we would like to propose that the term "posterior retinoschisis" is more appropriate than "macular retinoschisis" or "foveal retinoschisis." Although the BCVA in eyes with FD seemed to be poorer than that in eyes without FD, six eyes had a BCVA of better than 0.2, and the presence of FD could not be determined based only on visual acuity.

In 7 of the 16 eyes, OCT revealed the presence of a detached posterior hyaloid surrounding the macula, which may have widely stretched the posterior pole. The appearance of posterior vitreous adhesions over the macula was consistent with our experience of performing vitrectomies for retinal detachment associated with a macular hole[14] and a previous clinicopathological report,[15] which suggested that the posterior hyaloid might remain tightly attached to the macula, despite the presence of PVD in highly myopic eyes. Although PVD was not observed in the other nine eyes preoperatively, OCT examinations may be limited in detecting preretinal structures in highly myopic cases. In the present study, final reattachment was obtained in all 16 eyes, and no recurrences were observed in any eyes for over 6 months (the mean follow-up period was 23.3 months) after final surgery. This result suggests that the release of vitreous traction at the posterior pole may have an important role in the treatment of myopic RS and FS.

We performed vitrectomy, including vitreous cortex removal, in all eyes and internal limiting membrane (ILM) peeling in six eyes. All five eyes with RS and without FD achieved retinal reattachment after the initial vitrectomy. However, 3 of the 11 eyes with RS and FD required reoperation after the initial vitrectomy. In two of these three eyes, a full-thickness macular hole associated with posterior retinal detachment occurred about 1 month after vitrectomy with or without ILM peeling. The incidence of the development of macular hole retinal detachment seems to be higher than in previous reports,[3–7] in which most cases received ILM peeling. Kuhn[6] suggested that ILM may be responsible for macular detachment in highly myopic eyes. We also observed the proliferation of glial cells, which cause an abnormal ILM figure in highly myopic eyes.[14] ILM peeling may be highly beneficial for reducing the traction on the detached retina. However, the side effects of ILM peeling remain unknown. In addition, ILM peeling is technically difficult in highly myopic eyes, and ICG may be toxic to the neural retina as well as to the RPE.[16] The number of surgical reports remains insufficient, and we were able to obtain retinal reattachment in most of the eyes without ILM peeling. Thus, we were unable to conclude whether ILM peeling leads to a better anatomical prognosis. However, current techniques, such as TA-assisted vitrectomy or viscodissection, may be useful to avoid ILM peeling.

The role of gas tamponade in treatment is also uncertain. Gas tamponade can induce pneumatic displacement of outer-layer detachments and improve vision in retinoschisis associated with optic disc pits.[17] We expected intravitreal tamponade to have a similar effect in myopic eyes with RS and FD. However, intravitreal tamponade may push the subretinal fluid inside the limited area of the posterior staphyloma toward the weak point of the fovea, causing the formation of a macular hole. In two eyes with RS but without FD, retinal reattachment was obtained without using gas tamponade. Further study is needed to optimize surgical techniques.

Progression to a macular hole occurred preoperatively in 2 out of the 16 eyes and postoperatively in 3 out of 14 eyes. These eyes had relatively severe FD with posterior staphyloma prior to the development of a macular hole, and the BCVA of these eyes was worse than that of the others. These cases might have been at an advanced stage following the early development of a macular hole, similar to the two cases reported by Ikuno and Tano.[18] Patients and surgeons should regard this probable advanced stage with severe FD and poor vision as being equivalent to the early stage of macular hole retinal detachment when treating this condition.

Visual acuity improved or remained stable in all the eyes in the present study. Considering the poor prognosis of macular hole retinal detachment, vitrectomy using modern surgical techniques to induce PVD or to perform ILM peeling may be effective for the treatment of RS and/or FD in highly myopic eyes. However, further study is needed to select surgical indications and optimize surgical techniques to avoid complications, including macular hole.

References

1. Phillips CI. Retinal detachment at the posterior pole. Br J Ophthalmol 1958;42:749–753.
2. Takano M, Kishi S. Foveal retinoschisis and retinal detachment in severely myopic eyes with posterior staphyloma. Am J Ophthalmol 1999;128:472–476.
3. Ishikawa F, Ogino N, Okita K, et al. Vitrectomy for macular detachment without macular hole in highly myopic eyes. Atarashii Ganka (J Eye) 2001;18:953–956.
4. Kobayashi H, Kishi S. Vitreous surgery for highly myopic eyes with foveal detachment and retinoschisis. Ophthalmology 2003;110:1702–1707.
5. Kanda S, Uemura A, Sakamoto Y, Kita H. Vitrectomy with internal limiting membrane peeling for macular retinoschisis and retinal detachment without macular hole in highly myopic eyes. Am J Ophthalmol 2003;136:177–180.
6. Kuhn F. Internal limiting membrane removal for macular detachment in highly myopic eyes. Am J Ophthalmol 2003;135:547–549.
7. Ikuno Y, Sayanagi K, Ohji M, et al. Vitrectomy and internal limiting membrane peeling for myopic foveoschisis. Am J Ophthalmol 2004;137:719–724.
8. Baba T, Ohno-Matsui K, Futagami S, et al. Prevalence and characteristics of foveal retinal detachment without macular hole in high myopia. Am J Ophthalmol 2003;135:338–342.
9. Benhamou N, Massin P, Haouchine B, et al. Macular retinoschisis in highly myopic eyes. Am J Ophthalmol 2002;133:794–800.
10. Oshima Y, Ikuno Y, Motokura M, et al. Complete epiretinal membrane separation in highly myopic eyes with retinal detachment resulting from a macular hole. Am J Ophthalmol 1998;126:669–676.
11. Grigorian RA, Castellarin A, Fegen R, et al. Epiretinal membrane removal in diabetic eyes: comparison of viscodissection with conventional methods of membrane peeling. Br J Ophthalmol 2003;87:737–741.
12. Peyman GA, Cheema R, Conway MD, et al. Triamcinolone acetonide as an aid to visualization of the vitreous and the posterior hyaloid during pars plana vitrectomy. Retina 2000;20:554–555.
13. Polito A, Lanzetta P, Del Borrelo M, et al. Spontaneous resolution of a shallow detachment of the macula in a highly myopic eye. Am J Ophthalmol 2003;135:546–547.
14. Hirakata A. Retinal detachments and related eye diseases. In: Miyake Y, editor. Examination and diagnosis for vitreoretinal diseases. Textbook of lectures of lifelong education for the ophthalmologist. Tokyo: The Japan Ophthalmologist Association; 2002. p. 18–63.

15. Ishida S, Yamazaki K, Kawashima S, et al. Macular hole retinal detachment in highly myopic eyes: ultrastructure of surgically removed epiretinal membrane and clinicopathological correction. Retina 2000;20:176–183.
16. Gandorfer A, Haritoglou C, Gandorfer A, Kampik A. Retinal damage from indocyanine green in experimental macular surgery. Invest Ophthalmol Vis Sci 2003;44:316–323.
17. Lincoff H, Kreissig I. Optical coherence tomography of pneumatic displacement of optic disc pit maculopathy. Br J Ophthalmol 1998;82:367–372.
18. Ikuno Y, Tano Y. Early macular holes with retinoschisis in highly myopic eyes. Am J Ophthalmol 2003;136:741–744.

Jpn J Ophthalmol 2005;49:414–416

DOI 10.1007/s10384-004-0227-z

BRIEF COMMUNICATION

Multilayered Retinoschisis Associated with Optic Disc Pit

Akito Hirakata, Tetsuo Hida, Akiko Ogasawara, and Noriko Iizuka

Kyorin Eye Center, Kyorin University School of Medicine, Tokyo, Japan

Abstract

Background: Recently, optical coherence tomography (OCT) analysis has contributed greatly to the detection of posterior retinoschisis associated with optic disc pits. We report an unusual case of optic disc pit maculopathy.

Case: A 37-year-old woman with a multilayered structure of posterior retinoschisis associated with a very small, shallow optic disc pit was treated.

Observations: The patient came to our clinic after a few weeks of decreased vision in her right eye. Fundus examination showed a shallow macular detachment with a tiny, shallow pit at the temporal edge of the optic disc. OCT revealed an unusual multilayered structure of retinoschisis connected to the optic disc. We performed vitrectomy with induction of the posterior hyaloid separation and gas tamponade. After vitrectomy, OCT showed a marked fluid resolution in the retinoschisis, and the patient's vision improved rapidly.

Conclusion: The multilayered separation of retinoschisis can be caused by traction of the optic disc with a tiny, shallow pit at the temporal edge of the disc. **Jpn J Ophthalmol** 2005;49:414–416 © Japanese Ophthalmological Society 2005

Key Words: macular detachment, optical coherence tomography, optic disc pit, retinoschisis, vitrectomy

Introduction

Lincoff and coauthors[1] proposed that the retinal elevation that communicates with optic disc pits is a schisislike separation of the internal layers of the retina, based on a study of stereoscopic transparencies and visual fields performed in 1988. Outer layer detachment centered over the macula was suggested to be a secondary phenomenon. More recently, several authors have confirmed the two-layered structure of optic disc pit maculopathy using optical coherence tomography (OCT).[2,3] However, the source of the fluid in the retinoschisis cavity remains unclear.

We report a 37-year-old woman with an unusual multilayered structure of retinoschisis associated with a tiny, shallow pit at the temporal edge of the optic disc.

Received: November 8, 2004 / Accepted: November 17, 2004
Correspondence and reprint requests to: Akito Hirakata, Department of Ophthalmology, Kyorin University School of Medicine, 6-20-2 Shinkawa, Mitaka, Tokyo 181-8611, Japan
e-mail: hirakata@eye-center.org

Case Report

In April 2004, a 37-year-old Japanese woman was referred to our hospital after a few weeks of acute decreased vision in her right eye. Her best-corrected visual acuity (BCVA) was 0.5 OD and 1.2 OS. Her medical history was unremarkable. Fundus examination of the right eye revealed a serous detachment of the macula linked to the optic disc (Fig. 1A). The optic disc was slightly enlarged and exhibited a relatively large cupping with a tiny, shallow pit at the temporal edge of the disc (Fig. 1A). Optical coherence tomography (OCT, Humphrey Instruments, San Leandro, CA, USA) disclosed a multilayered separation of the neurosensory retina between the optic disc and the fovea (Fig. 1B, C). The irregular split in several layers of the papillomacular area was unusual in its appearance and in its association with the optic disc pit. A lamellar break of the inner layer and retinoschisis in the outer layer of the sensory retina were present around the center of the macula. Fluorescein angiography showed a weak leakage from the retinal small vessels beside the optic disc and late staining of the optic

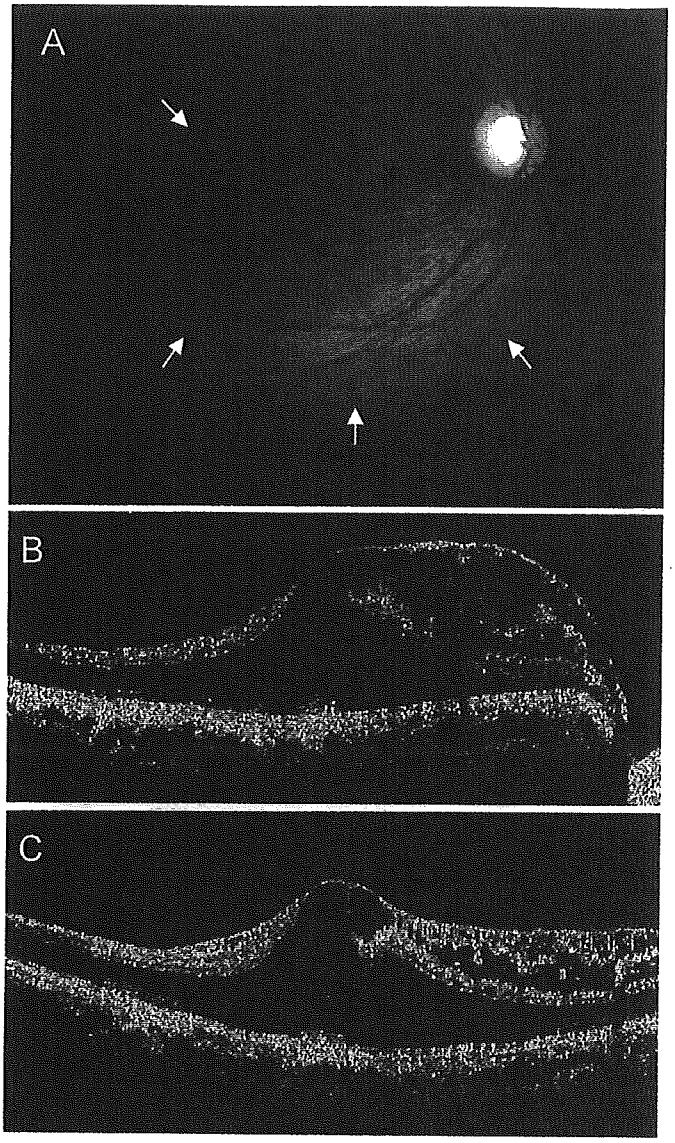

Figure 1A–C. Preoperative fundus findings (**A**) and cross-sectional optical coherence tomography (OCT) images (**B, C**). **A** The patient's visual acuity was 0.5 OD. A retinoschisis involving the macular and papillomacular areas is visible (*arrows*). A small, shallow, grayish pit is present at the inferotemporal margin of the slightly enlarged disc, with large cupping. **B** A horizontal cross-sectional OCT image shows the multilayered structure of the retinoschisis connected to the optic disc. The irregular split in several layers of the papillomacular area was unusual in its appearance and association with the optic disc pit (scan length, 10mm). **C** A vertical cross-sectional OCT image shows the irregular splitting of the superficial sensory retina (scan length, 10mm).

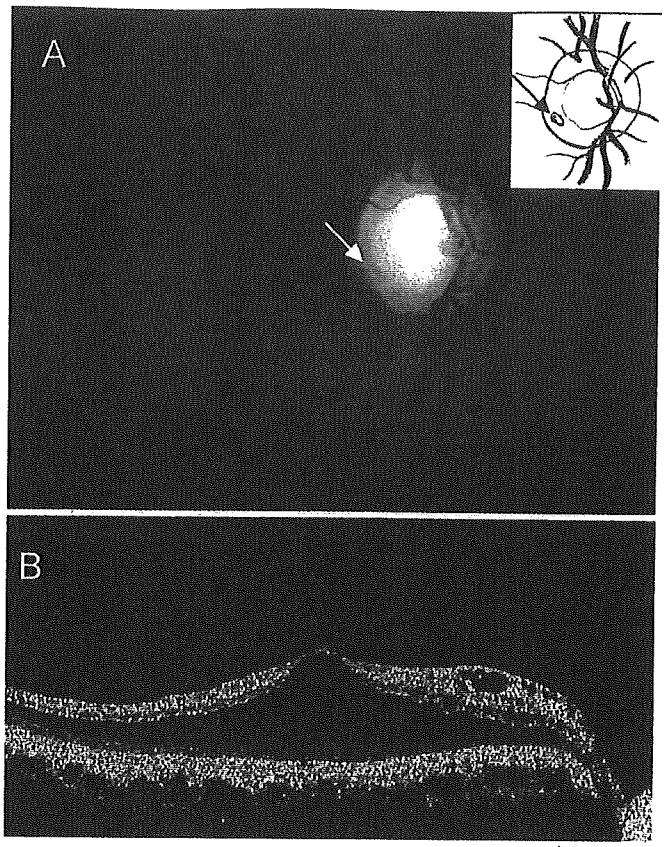

Figure 2A, B. Two-month postoperative optic disc findings (**A**) and cross-sectional OCT images (**B**). **A** The macular elevation is markedly reduced. A small, shallow, grayish pit is present at the inferotemporal margin of the optic disc (*arrow*). *Inset* shows a schematic drawing of the optic disc pit. **B** OCT shows the marked reduction of the irregular split in several layers of the superficial neurosensory retina in the papillomacular area. The patient's visual acuity was 1.2, although the macular outer retinoschisis persisted (scan length, 10mm).

disc. After two months of observation, the patient complained of a worsening in her central vision and metamorphopsia in her right eye. We decided to perform vitrectomy to improve her visual acuity. Advanced vitreous syneresis, but no posterior vitreous detachment, was observed during the operation. Triamcinolone acetonide was used intraoperatively to highlight the posterior hyaloid membrane. The separation of the posterior hyaloid was smoothly performed, even though the adhesion of the posterior hyaloid was very tight at the anterior border of the pit at the temporal edge of the optic disc. Fluid–air exchange was performed using a gas tamponade with 20% sulfur hexafluoride (SF_6). The patient was maintained in a postoperative face-down position for 1 week. Two weeks postoperatively, the patient's BCVA was 0.9, and the macular elevation was markedly reduced. OCT showed the marked reduction of the irregular split in several layers of the superficial neurosensory retina in the papillomacular area. Two months postoperatively, the BCVA improved to 1.2, with decreased residual retinoschisis of the posterior neurosensory retina (Fig. 2A, B).

Discussion

Recent OCT findings support the concept of a bilaminar structure in which a macular detachment develops secondarily to a preexisting retinoschisis, consisting of severe outer retinal edema.[2,3] In previous reports, the retinoschisis

Jpn J Ophthalmol
Vol 49: 414–416, 2005

cavities have been located deeper, at the outer plexiform layer, compared with that in the present case. The present patient exhibited a multilayered separation and severe edema. The separation in the more superficial part seemed to be at the neurofiber layers, between the optic disc and the fovea. The shape and position of the retinoschisis in the outer layer of the sensory retina around the center of the macula were similar in appearance to that of retinoschisis usually seen in optic disc pit maculopathy. The difference in the present case might have been caused by the shape and the position of the pit. The pit was atypically small and seemed to be a partial defect of the neurofiber layer inside the optic disc. Todokoro and Kishi[4] reported a case with a split in several layers of the papillomacular area associated with an optic disc pit. Using OCT analysis, they observed that the optic disc pit was not a true pit, but a cystic cavity covered by a superficial layer of the optic disc. Several variations in the structure or position of a pit in the optic disc may result in the different OCT appearances of the maculopathy. The vision of the present patient relatively acutely decreased but was restored soon after the surgery. This clinical course of visual acuity in the present patient was also different from that usually observed in patients with optic disc pit maculopathy.

Based on OCT examinations and experience in performing vitrectomies,[4] several authors have suggested that posterior vitreous traction may have an important role in the pathogenesis of optic pit maculopathy. In this case, the vitrectomy reduced the serous detachment, leading to an improvement in the patient's BCVA. During the vitrectomy, the posterior hyaloid was tightly attached to the anterior edge of the tiny shallow pit at the temporal edge of the optic disc. The late staining at the optic disc and the weak leakage from the small retinal vessels during the fluorescein angiography may have been caused by vitreous traction at the optic disc. Posterior vitreous traction may have introduced the fluid from the shallow pit at the temporal edge of the optic disc to the neurosensory retina, causing the irregular split in several layers of the papillomacular area.

Spaide and coauthors[5] reported a 29-year-old patient with a macular schisis without an optic disc pit. OCT findings showed a thin sheet of tissue with a small break or fenestration on the optic nerve. The abnormal structure on the optic disc or a preexisting tight adhesion between the posterior vitreous, including abnormal membranelike tissue, and the optic disc might have produced the retinoschisis, even if an optic disc pit was not present. If the fluid in the unique retinoschisis in the present case originated from the unusually small and shallow pit at the edge of the optic disc, the fluid in the two-layered structure of a typical optic disc pit maculopathy may arise from a much deeper level, possibly the subarachnoid space.

References

1. Lincoff H, Lopez R, Kreissig I, et al. Retinoschisis associated with optic nerve pits. Arch Ophthalmol 1988;106:61–67.
2. Rutledge BK, Puliafito CA, Duker JS, Hee MR, Cox MS. Optical coherence tomography of macular lesions associated with optic nerve head pits. Ophthalmology 1996;103:1047–1053.
3. Krivoy D, Gentile R, Liebmann JM, Stegman Z, Walsh JB, Ritch R. Imaging congenital optic disc pits and associated maculopathy using optical coherence tomography. Arch Ophthalmol 1996;114:165–170.
4. Todokoro D, Kishi S. Reattachment of retina and retinoschisis in pit-macular syndrome by surgically-induced vitreous detachment and gas tamponade. Ophthalmic Surg Lasers 2000;31:233–235.
5. Spaide RF, Costa DL, Huang SJ. Macular schisis in a patient without an optic disk pit: optical coherence tomography findings. Retina 2003;23:238–240.

Cell Tissue Res
DOI 10.1007/s00441-005-0122-z

REGULAR ARTICLE

Yasuko Yamaguchi · Takashi Watanabe ·
Akito Hirakata · Tetsuo Hida

Localization and ontogeny of aquaporin-1 and -4 expression in iris and ciliary epithelial cells in rats

Received: 7 August 2005 / Accepted: 8 November 2005

Abstract The precise localization of aquaporin (AQP)1 and AQP4 was studied in iris and ciliary epithelial cells, in both mature and developing rats, to elucidate the molecular mechanisms underlying aqueous humor balance. Anterior segments of eyes dissected from embryonic day (E)13, E15, E18, and E20, postnatal day (P)0, P7, and P14, and postnatal week 8 rats were subjected to immunofluorescence analysis with AQP isoform-specific antibodies. In adult rat eye, AQP1 was localized to the apical and basolateral plasma membranes of iris epithelial cell layers and of anterior ciliary non-pigmented epithelial (NPE) cells. Conversely, AQP4 was localized to the basolateral plasma membrane of NPE cells in ciliary epithelium and the posterior iris. Developmentally, AQP1 was detected as early as E15 in immature iris and ciliary epithelial cells, and expression persisted throughout development up to adulthood. In contrast, AQP4 was first observed at P7 in the developing pars plicata, and the AQP4-positive area gradually spread to cover the entire pars plicata as development proceeded. These findings indicate that both AQP1 and AQP4 contribute to aqueous humor secretion in the rat eye, thereby maintaining proper intraocular pressure. Moreover, AQP appears to play a major role in aqueous humor secretion in early eye development. This study thus provides a basis for understanding the molecular mechanisms of aqueous humor secretion in pathological and physiological conditions.

Keywords Aquaporin · Iris epithelium · Ciliary epithelium · Aqueous humor · Fluid transport · Immunofluorescence analysis · Rat (Sprague Dawley)

Y. Yamaguchi (✉) · A. Hirakata · T. Hida
Department of Ophthalmology,
Kyorin University School of Medicine,
6-20-2 Shinkawa,
Mitaka, Tokyo, 181-8611, Japan
e-mail: yamaguchi@eye-center.org
Tel.: +81-422-475511

T. Watanabe
Laboratory Medicine,
Kyorin University School of Medicine,
6-20-2 Shinkawa,
Mitaka, Tokyo, 181-8611, Japan

Introduction

Aquaporins (AQPs) are molecular water channels localized in plasma membranes in animals, plants, and microorganisms (Chrispeels and Agre 1994; Calamita et al. 1995). In mammalian cells, 11 isoforms of AQPs (AQP0–AQP10) have been identified to date (Matsuzaki et al. 2002; Verkman 2003). AQPs are present in cells requiring either rapid bulk transport of fluid or transport of fluids against an insufficient osmotic pressure gap. AQPs allow efficient transport of fluid, thereby contributing to the maintenance of proper organ function (Stamer et al. 1994; Patil et al. 1997a; Hamann et al. 1998).

Of the 11 AQP isoforms, AQP0, AQP1, AQP3, AQP4, and AQP5 have been shown to be localized in mammalian eyes (Patil et al. 1997a; Hamann et al. 1998; Verkman 2003). AQP1 and AQP4 are localized in ciliary epithelial cells and appear to be involved in aqueous humor secretion (Patil et al. 1997a, 2001; Hamann et al. 1998; Zhang et al. 2002; Verkman 2003). Within the eye, the watery aqueous humor plays important roles in maintaining proper visual function. Aqueous humor generates a suitable intraocular pressure (IOP) and also conveys nutrients and metabolic waste to and from avascular intraocular tissues such as the lens (Caprioli 1992). Moreover, the aqueous humor appears essential in normal eye development (Reichman and Beebe 1992). Aqueous humor is also important ophthalmologically, as impairments in water dynamics can result in eye disorders such as glaucoma. The molecular

mechanisms involved in aqueous humor dynamics, however, remain largely unclear. The present study has therefore attempted to identify localization of AQP1 and AQP4 in iris and ciliary epithelial cells in rats by using immunocytochemical methods. Developmental expression of AQP1 and AQP4 in rat iris and ciliary epithelial cells has also been examined from embryonic to postnatal stages. This is the first precise analysis of AQP1 and AQP4 localization in iris and ciliary epithelial cells in both mature and developing rats.

Materials and methods

Animals

Timed-pregnant and postnatal Sprague-Dawley rats were obtained from Clea Japan (Tokyo, Japan). Birth usually occurred on embryonic day (E)22, which was considered as postnatal day (P)0. Samples taken on E13, E15, E18, and E20 from fetal rats, on P0, P7 and P14 from postnatal rats, and at postnatal week (PW)8 from adult female rats were

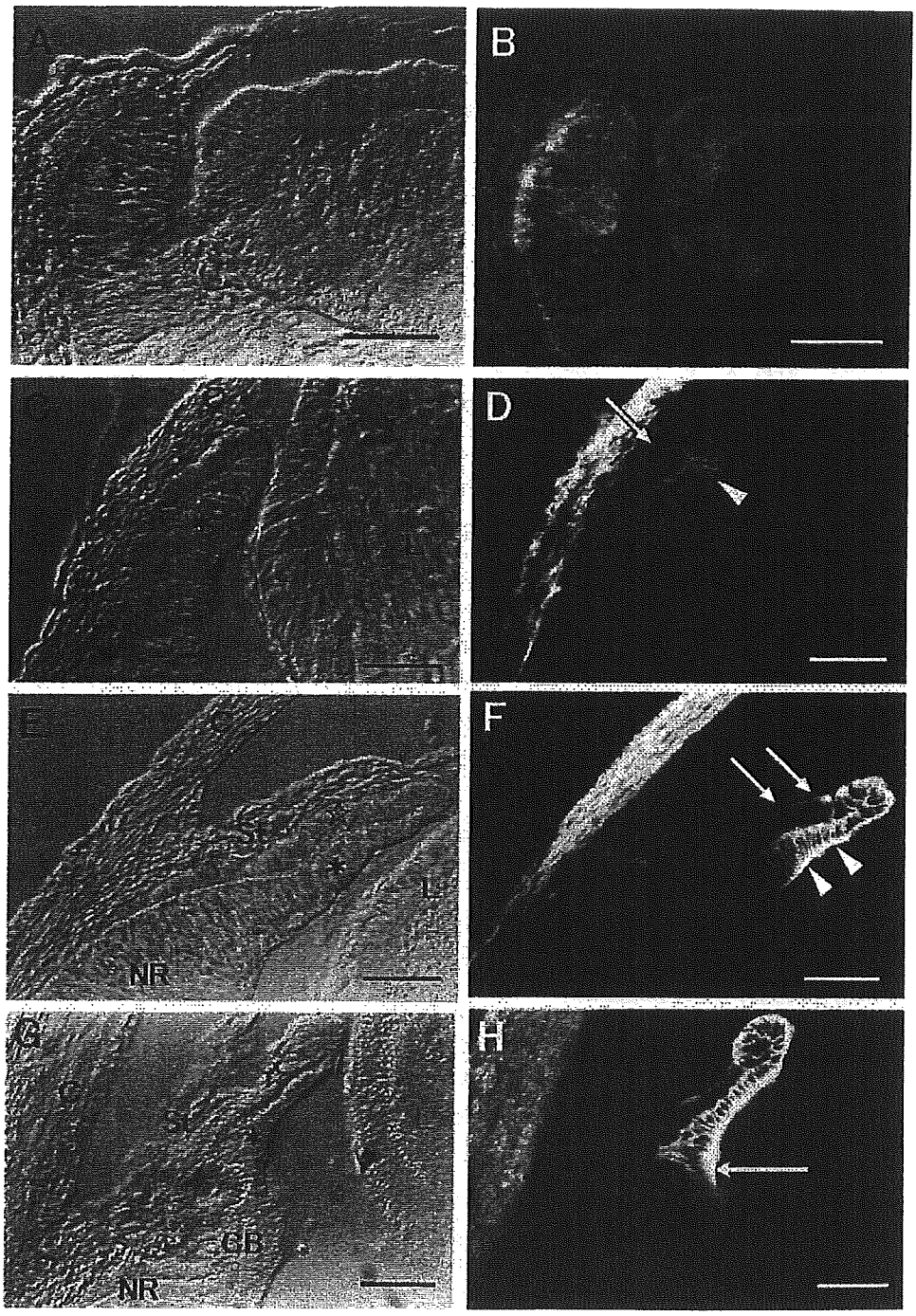

Fig. 1 AQP1 immunolocalization in iris and ciliary epithelial cells in embryonic rat eyes (*C* cornea, *L* lens, *CB* ciliary body, *NR* neural retina, *asterisks* inner plate, *stars* outer plate, *St* iris and ciliary stroma). Vertical sections through developing eyes dissected from E13, E15, E18, and E20 rats were immunostained with anti-AQP1 antibody followed by FITC-labeled swine anti-rabbit immunoglobulin and then photographed using Nomarski (**a, c, e, g**) and fluorescence (**b, d, f, h**) optics. At E13 (**a, b**), no definitive AQP1–IR was observed in either inner or outer plates of the optic cup. AQP1–IR first appeared at E15 (**c, d**). At E15 and E18 (**e, f**), AQP1–IR was confined to the anterior ends of the developing optic cup. Within this region, the optic cup inner plate (**d, f,** *arrowheads*) showed more intense AQP1–IR than the outer plate (**d, f,** *arrows*). The intensity of AQP1–IR increased dramatically as development proceeded from E15 (**d**) to E18 (**f**). At E20 (**g, h**), AQP1–IR was observed in the most anterior region of the ciliary body (**h,** *arrow*) in addition to the entire iris, and AQP1–IR intensity was significantly higher than at E15 or E18. In the cornea, AQP1–IR was first observed at E15 (**d**) and persisted throughout the embryonic stages (**f, h**). *Bars* 25 μm

subjected to immunohistochemical analysis. All animal care and tissue collection procedures were performed in accordance with the ARVO Statement for the Use of Animals in Ophthalmic and Vision Research.

Preparation of eye specimens

Embryos (E13, E15, E18, and E20) were removed after pregnant Sprague-Dawley rats has been killed by cervical dislocation under deep anesthesia induced by diethyl ether. Eyes were immediately enucleated and immersion-fixed in 4% paraformaldehyde in 0.1 M phosphate buffer (PB, pH 7.4) for 2 h at 4°C. Postnatal rats (P0 and P7) were sacrificed by decapitation. Eyes were immediately enucleated, and the anterior segments were dissected. Resultant eye tissues were immersion-fixed in a similar manner to embryonic eyes. For P14 and PW8 rats, animals were perfused transcardially with 0.01 M phosphate-buffered saline (PBS, pH 7.4) followed by ice-cold fixative containing 4% paraformaldehyde in PB under deep anesthesia induced by diethyl ether. Eyes were enucleated and processed in a similar manner to those from P0 and P7 rats. All tissue samples were subsequently cryoprotected by using a graded series of sucrose in PBS at 4°C, embedded in OCT compound (Sakura Finetechnical, Tokyo, Japan), and frozen. Frozen sections (6 μm) were cut in an HM500 cryostat (Zeiss) and transferred onto 3–aminopropyltrethoxy–silane–coated slides. A hydrophobic ring was drawn around sections by using a PAP pen (Daido Sangyo, Tokyo, Japan). Sections were then air-dried for 1 h at room temperature.

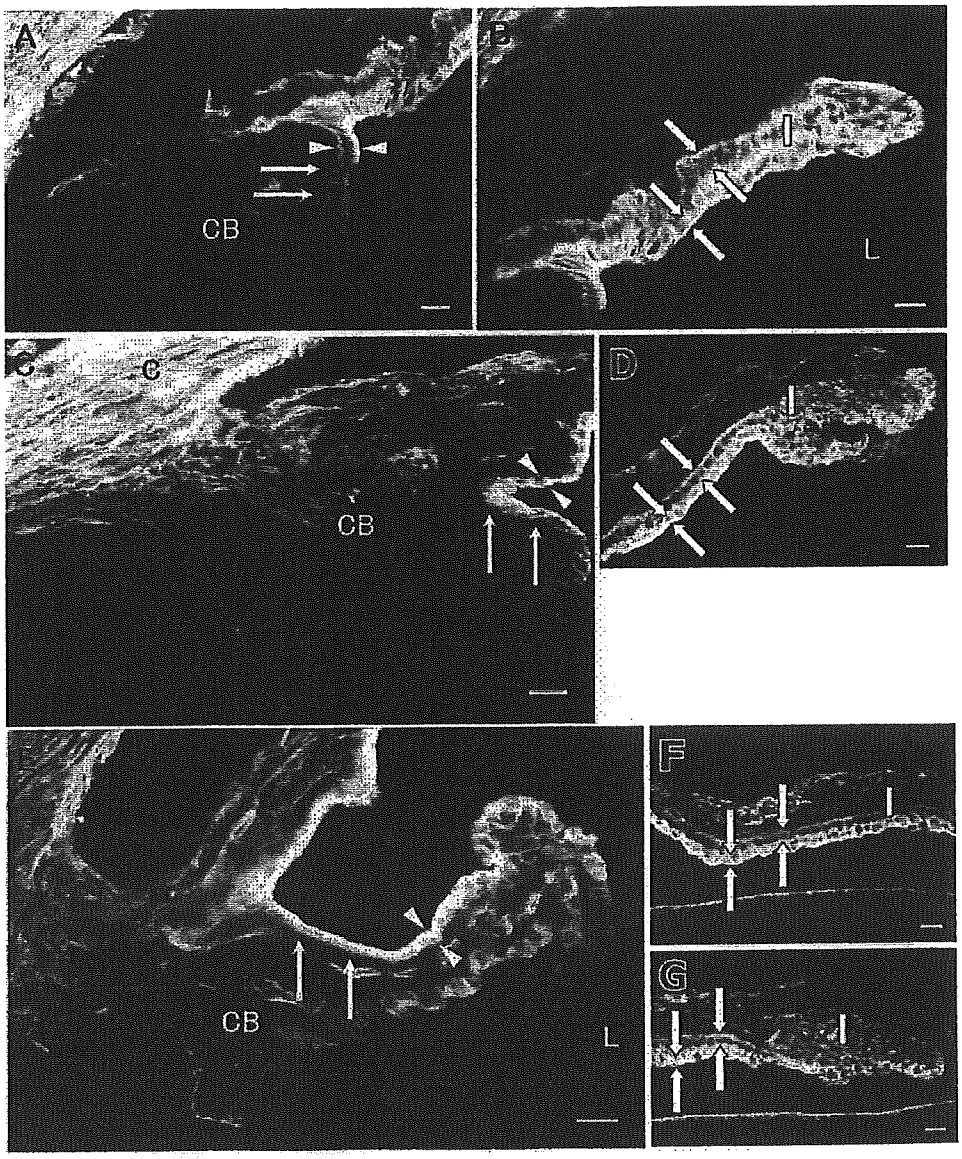

Fig. 2 AQP1 immunolocalization in iris and ciliary epithelial cells of postnatal rat eyes (*C* cornea, *CB* ciliary body, *I* iris, *L* lens). Vertical sections through anterior ocular segments dissected from P0, P7 and P14 rats were immunostained with anti-AQP1 antibody followed by FITC-labeled swine anti-rabbit immunoglobulin and then photographed under fluorescence optics. At P0 (**a, b**), both apical and basolateral plasma membranes of the inner plate cells corresponding to NPE cells in the anterior region of the ciliary body, displayed AQP1–IR (**a**, *arrowheads*), whereas outer plate cells corresponding to PE cells were AQP1-negative (**a**, *arrows*). In both layers of iris epithelial cells, both apical and basolateral plasma membranes were stained (**b**, *arrows*). At P7 (**c, d**) and P14 (**e–g**), the AQP1–IR pattern in the ciliary and iris epithelium was similar to that at P0 (**c, e**: *arrowheads* NPE, *arrows* PE; **d, g**: *arrows* anterior region of iris; **f**: *arrows* medial region of iris). Cornea was AQP1-positive throughout the postnatal stages (**c**). *Bars* 10 μm

Antibodies

Rabbit anti-rat AQP1 and AQP4 antibodies (Chemicon, Temecula, Calif.) were used. The specificities of these antibodies have been extensively examined by Western blot analysis in rodents (AQP1: Ward et al. 2001; Frigeri et al. 2004, AQP4: Yamamoto et al. 2001; Dalloz et al. 2003).

Immunofluorescence staining

For immunofluorescence staining, sections were rinsed in PBS (3×5 min each), treated with 10% normal swine serum in PBS for 10 min, and then incubated overnight at 4°C with either anti-AQP1 antibody (diluted 1:100) or anti-AQP4 antibody (diluted 1:20). All sections were rinsed in PBS (3×5 min each) and then incubated in swine anti-rabbit immunoglobulin coupled to fluorescein isothiocyanate (FITC; diluted 1:100; DakoCytomation, Glostrup, Denmark) for 1 h at room temperature. The above antibodies were all diluted in PBS containing 4% fetal calf serum, 0.1% sodium azide, and 0.1% Triton X–100. Sections were again rinsed in PBS (3×5 min each), mounted in glycerol containing 0.1% paraphenylenediamine to prevent bleaching, and examined with an Axioplan fluorescence microscope (Zeiss). Photomicrographs were taken by using 400 ASA Tri-X film (Kodak, Rochester, N.Y.).

To test the specificity of immunoreactivity (IR), control sections were processed in the same manner as described above, except that anti-AQP1 and anti-AQP4 antibodies were replaced with primary antibodies pre-adsorbed with either AQP1 or AQP4 oligopeptide (50 μg/ml diluted antibody; Chemicon), respectively, at 4°C for 4 h. These

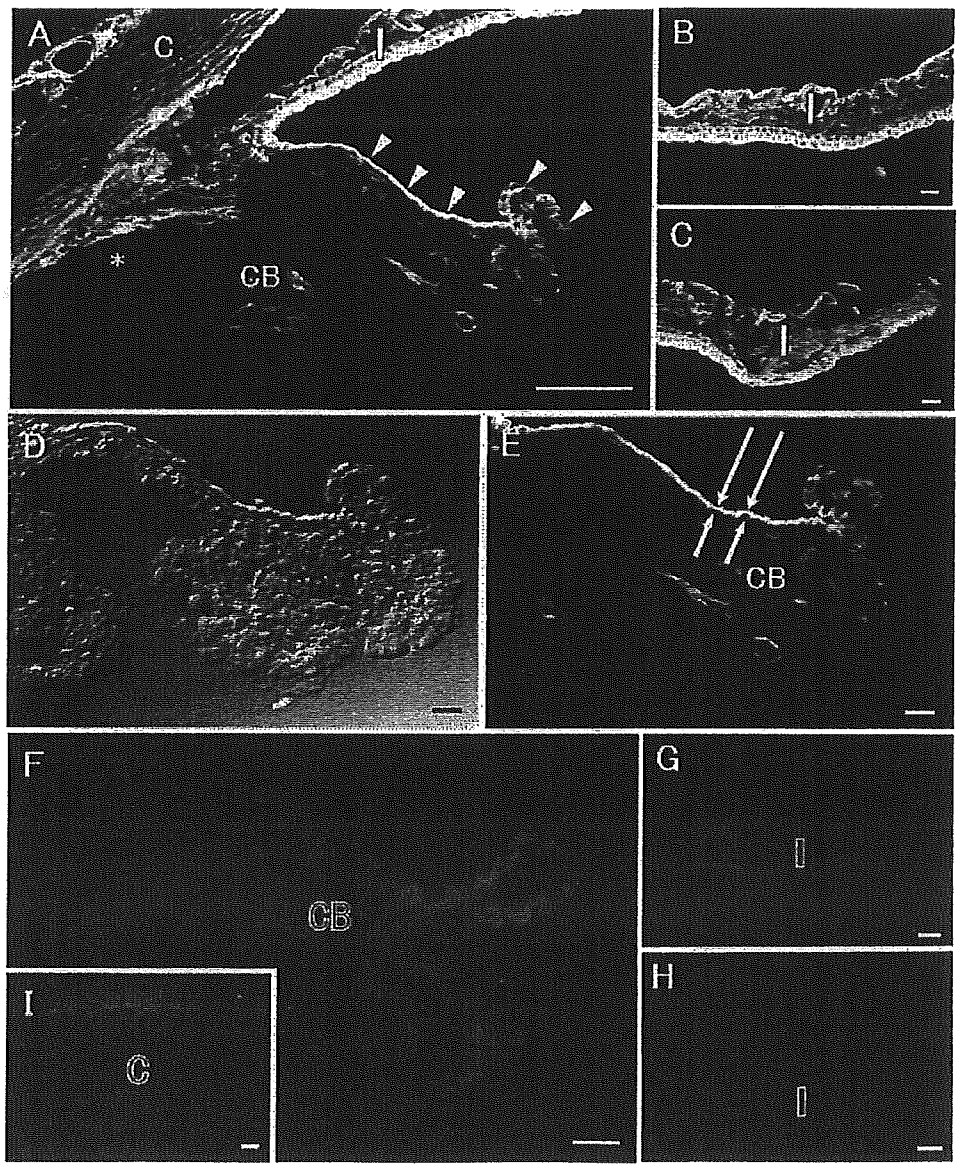

Fig. 3 AQP1 immunolocalization in iris and ciliary epithelial cells of PW8 rat eyes (*C* cornea, *CB* ciliary body, *I* iris, *asterisk* pars plana). Vertical sections through anterior ocular segments dissected from PW8 rats were immunostained with anti-AQP1 antibody followed by FITC-labeled swine anti-rabbit immunoglobulin and then photographed under Nomarski (**d**) and fluorescence (**a–c, e**) optics. AQP1–IR for epithelial cells in the iris (**a** posterior region, **b** medial region, **c** anterior region) and ciliary body (**a, d, e**) basically resembled that seen during developmental stages. In iris epithelial cells, both layers were AQP1-positive. In ciliary epithelial cells, only NPE cells localized anterior to the pars plicata were stained (**a**, *arrowheads*). AQP1–IR intensity was higher on the basolateral side (**e**, *long arrows*) than on the apical side (**e**, *small arrows*). In the remaining pars plicata and pars plana (**a**, *asterisk*), neither NPE cells nor PE cells were stained. Cornea was also AQP1-positive (**a**). **f–i** Pre-adsorption of anti-AQP1 antibody with antigenic peptide. PW8 rat anterior ocular segments were immunostained with anti-AQP1 antibody pre-adsorbed with AQP1-specific antigenic peptide. In ciliary (**f**) and iris (posterior region is not shown; **g** medial region, **h** anterior region) epithelium and in cornea (**i**), the AQP1–IR observed in **a–c** was completely abolished. *Bars* 10 μm

oligopeptides were equivalent to those used as immunogens to raise anti-AQP1 and anti-AQP4 antibodies.

Results

Prenatal AQP1 immunolocalization in iris and ciliary epithelial cells

At E13, no definitive AQP1–IR was observed in either the inner or outer plates of the optic cup (Fig. 1a,b). AQP1–IR first appeared at E15. At this stage, AQP–IR was confined to the anterior margin of the optic cup (Fig. 1c,d), where the inner plate of the optic cup showed more intense AQP1–IR than the outer plate, despite the outer and inner plates representing continuous tissues. In this region, AQP1–IR was observed all around the cell membrane. At E18, the anterior tip of the optic cup continued to grow along the lens anteriorly (Fig. 1e). At the same time, the iris and ciliary stroma began to form. The posterior part of the inner plate thickened markedly to form the neurosensory retina. AQP1–IR in the inner plate was more intense at E18 than at E15 (Fig. 1f). AQP1–IR in the outer plate also became more intense than at E15. However, AQP1–IR at E18 was again much more intense in the inner plate than in the outer plate. In the inner plate, although both apical and basolateral plasma membranes were stained, AQP1–IR intensity was higher on the basolateral side. At E20, when the iris became distinguishable from the ciliary body, AQP1–IR was observed in the most anterior region of the

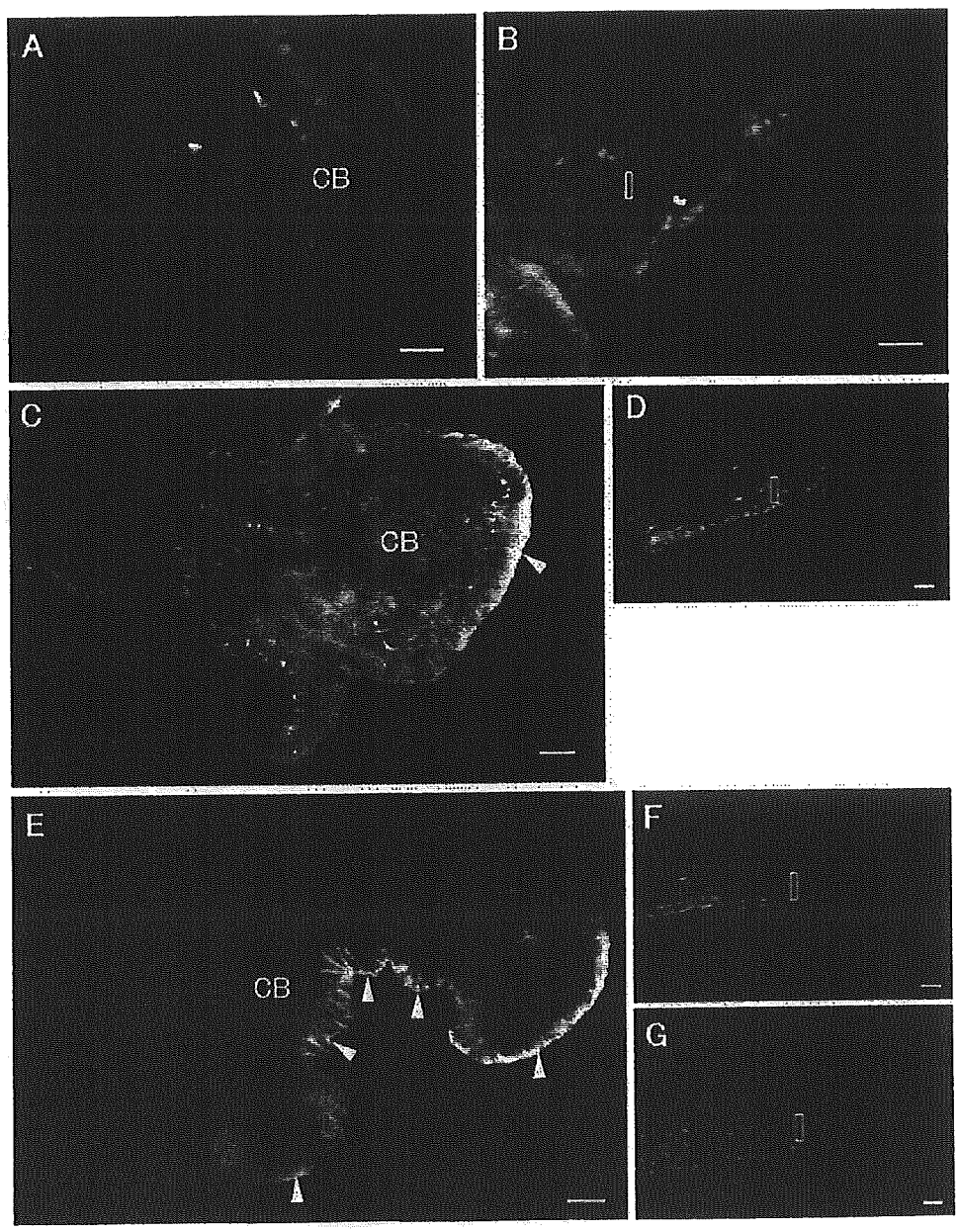

Fig. 4 AQP4 immunolocalization in iris and ciliary epithelial cells of postnatal rat eyes (*CB* ciliary body, *I* iris). Vertical sections through anterior ocular segments dissected from P0 (**a, b**), P7 (**c, d**), and P14 (**e–g**) rats were immunostained with anti-AQP4 antibody followed by FITC-labeled swine anti-rabbit immunoglobulin and then photographed under fluorescence optics. Little AQP4–IR was present in the ciliary body (**a**) or iris (**b**) at P0. Weak AQP4–IR was first observed on NPE cells of the immature pars plicata (**c**, *arrowhead*) at P7. AQP4–IR was more prominent at P14 than at P7 (**e**, *arrowheads*). At both P7 and P14, both iris epithelial layers (**d, g** anterior region; **f** medial region) were AQP4-negative. *Bars* 10 μm

ciliary body, in addition to the entire iris (Fig. 1g,h). At this stage, AQP1–IR intensity was significantly higher than at E15 or E18. AQP1–IR in the cornea was first seen at E15 and was observed throughout the embryonic stages (Fig. 1d,f,h).

Postnatal AQP1 immunolocalization in iris and ciliary epithelial cells

The iris and ciliary body remained structurally immature at birth (Fig. 2a). At P0, fold formation in the ciliary body remained incomplete. However, the ciliary body was more readily distinguishable from the iris at this stage than in the embryonic stages. In the anterior region of the ciliary body, both apical and basolateral plasma membranes of the inner plate cells corresponding to non-pigmented epithelial (NPE) cells, displayed AQP1-IR, whereas outer plate cells corresponding to pigmented epithelial (PE) cells showed no AQP1–IR (Fig. 2a). In both layers of the iris epithelial cells that were continuous with ciliary epithelial cells, both apical and basolateral plasma membranes were stained, but AQP1–IR intensity was lower in the anterior part of iris epithelium than in the posterior part (Fig. 2b). As development proceeded, the ciliary body formed more complex folds (Fig. 2c,e), and the iris extended at P7 and P14 (Fig. 2d,f,g). Patterns of AQP1–IR in the ciliary (Fig. 2c,e) and iris (Fig. 2d,f,g) epithelium at P7 and P14 basically resembled that at P0. AQP1–IR in the cornea was also observed throughout the postnatal stages (Fig. 2c).

At PW8, when development of the eyeball had been completed, AQP1–IR for epithelial cells in the iris and ciliary body was basically equivalent to that seen during the developmental stages. In iris epithelial cells, both layers were AQP1-positive (Fig. 3a–c). However, AQP1–IR was more intense in posterior epithelium compared to anterior epithelium. In ciliary epithelial cells, only NPE cells localized anterior to the pars plicata were stained (Fig. 3a). The intensity of AQP1–IR was higher on the basolateral side than on the apical side, again resembling observations made during development (Fig. 3d,e). In the remaining pars plicata and pars plana, neither NPE cells nor PE cells were stained (Fig. 3a). AQP1–IR was also observed in the cornea (Fig. 3a).

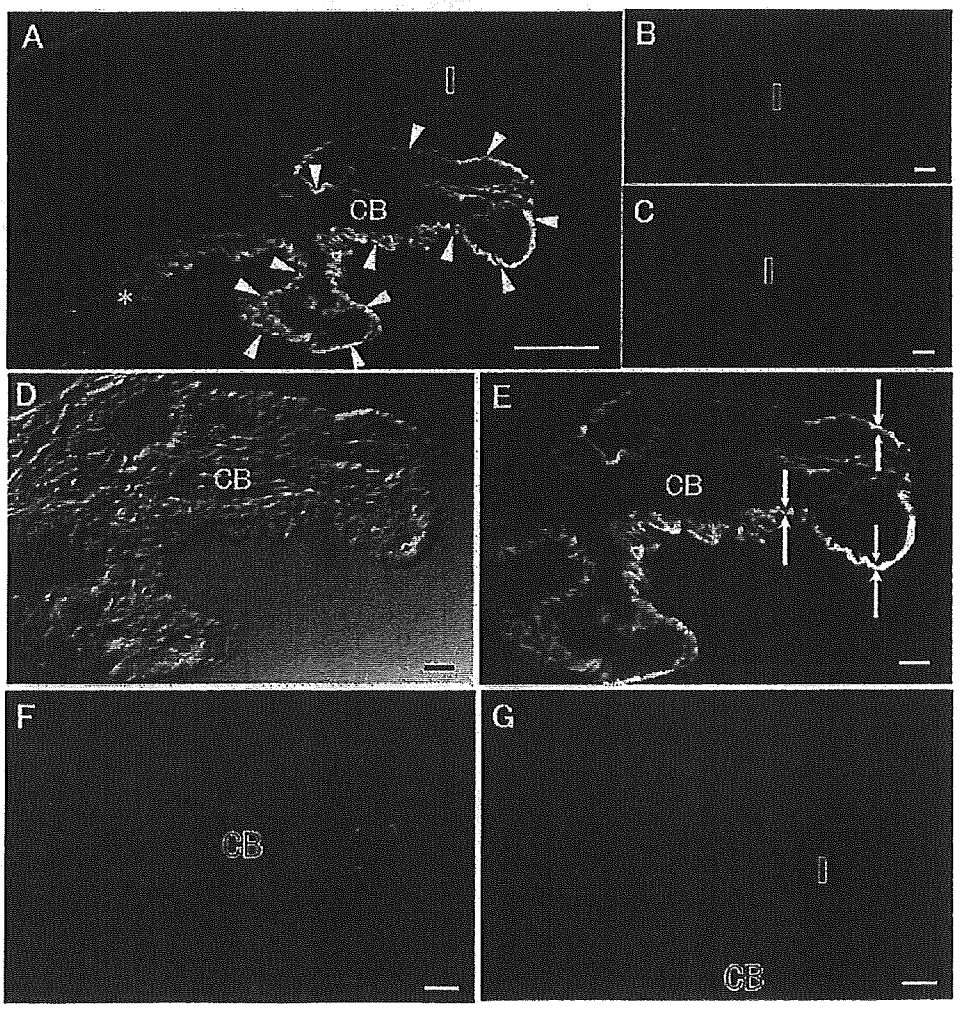

Fig. 5 AQP4 immunolocalization in iris and ciliary epithelial cells of PW8 rat eyes (*CB* ciliary body, *I* iris, *asterisk* pars plana). Vertical sections through anterior ocular segments dissected from PW8 rats were immunostained with anti-AQP4 antibody followed by FITC-labeled swine anti-rabbit immunoglobulin and then photographed under Nomarski (**d**) and fluorescence (**a–c, e**) optics. AQP4–IR was observed in the entire pars plicata region of the ciliary body (**a**, *arrowheads*). In this region, only NPE cells were AQP4-positive, not PE cells. AQP4-IR was observed only on the basolateral plasma membrane (**e**, *large arrows*), and the apical side was AQP4-negative (**e**, *small arrows*). In contrast, the pars plana region of the ciliary body did not show any significant AQP4–IR (**a**, *asterisk*). In the iris (**a**, posterior region; **b**, medial region; **c**, anterior region), only the posterior region continuous with NPE cells displayed weak AQP4–IR (**a**). **f–g** PW8 rat anterior ocular segment stained with anti-AQP4 antibody preadsorbed with antigenic peptide. Note that the AQP4–IR in ciliary and iris epithelium seen in **a** was completely abolished (**f**, ciliary body; **g**, posterior region of iris). *Bars* 10 μm